A　死亡2.5日後の頭部T2強調冠状断像　　B　解剖

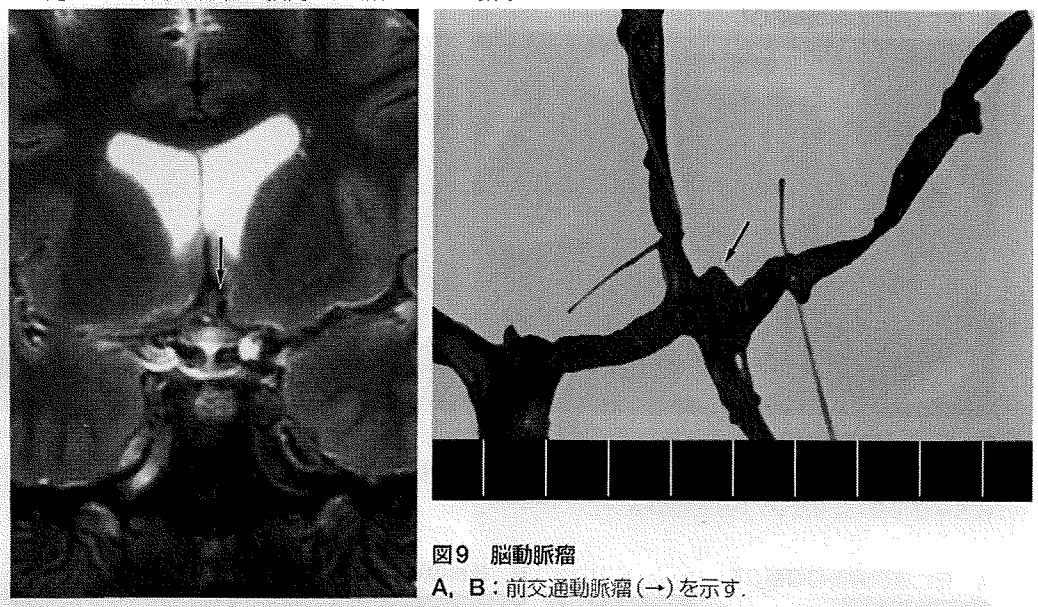

図9　脳動脈瘤
A, B：前交通動脈瘤(→)を示す.

A, B死亡確認直後の胸部CT
A　通常のCT　　B　高分解能CT

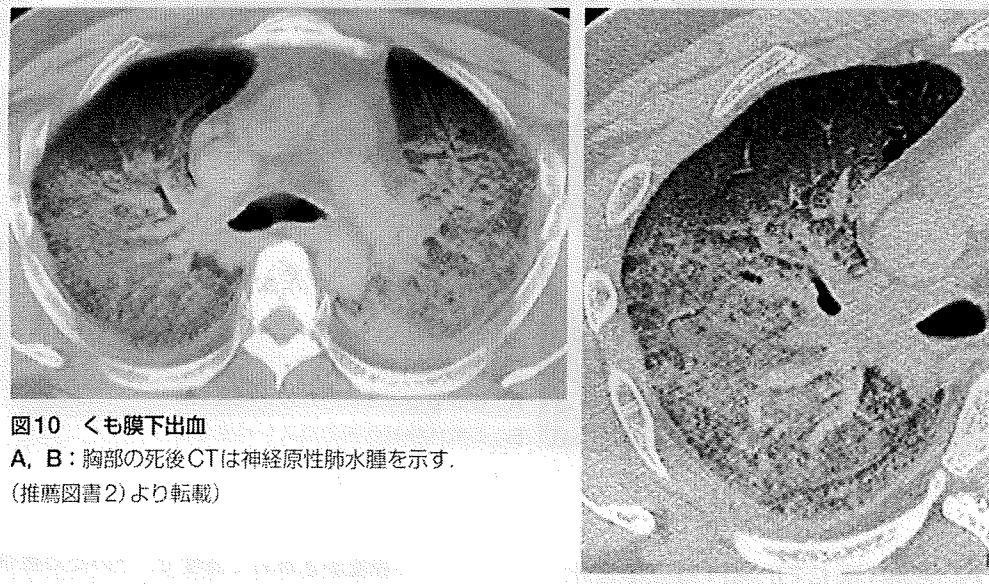

図10　くも膜下出血
A, B：胸部の死後CTは神経原性肺水腫を示す.
(推薦図書2)より転載)

る. 生きているヒトのCT上, 肝血管内ガスと言えば門脈ガスを指すが, 死後CTでは門脈ガスと肝静脈ガスの2種類がある. 門脈ガスは, ショック～心肺停止による循環障害が起こす腸管粘膜損傷と, アンビューバッグを用いた換気が起こす消化管拡張が原因となり, 消化管内腔のガスが門脈に流入したものである. 肝静脈ガスは, 心大血管内ガスの逆流による(心肺蘇生術中に超音波検査で肝を観察すると, 無数のガス粒が肝静脈の腹側壁に沿って末梢へ移動していることがわかる). 門脈ガスと肝静脈ガスは併存していることが多い(図13)が, 肝血管内ガスが少量であれば, どちらか区別がつかない. 肝以外に, 膵, 腎, 脾実質の血管内ガスも, 早期死後CTで既に出現していることが少なくない.

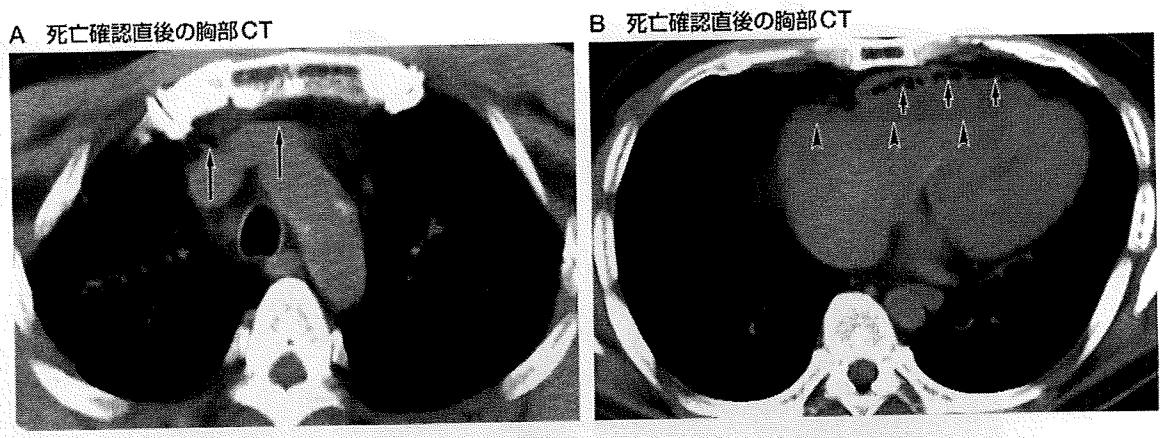

図11 心大血管内ガス
A, B：鎖骨下・腕頭静脈内のガス（A：→）と右心房・右心室自由壁直下のガス（B：→）を示す．Bでは，心臓内腔の高吸収水平面形成（血液就下）（→）も認める．

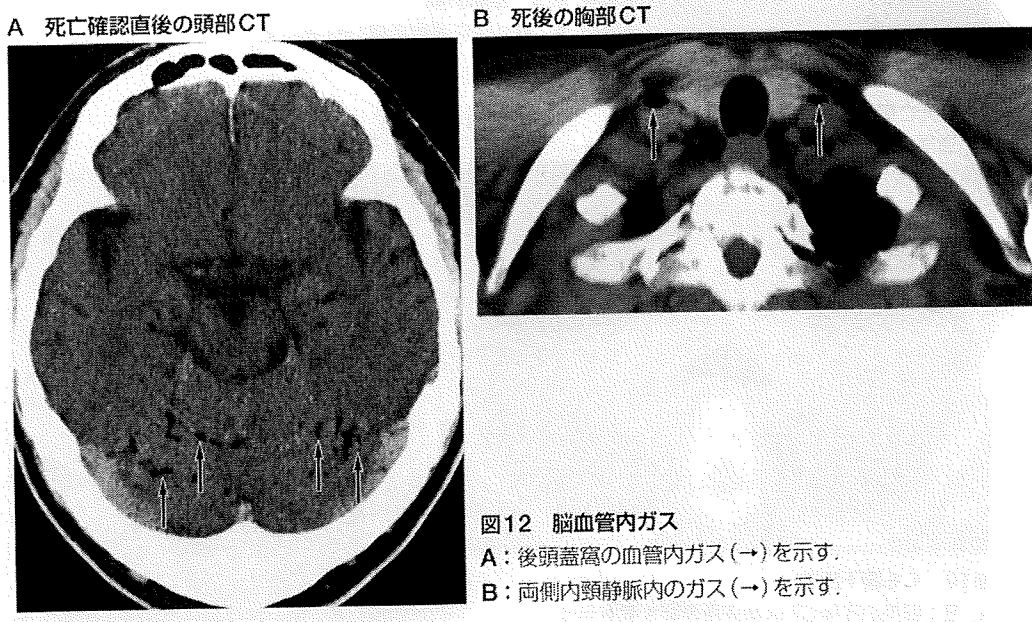

図12 脳血管内ガス
A：後頭蓋窩の血管内ガス（→）を示す．
B：両側内頸静脈内のガス（→）を示す．

8. 早期死後CTにおける死後変化

1）胸　部

a. 血液就下

急性死の場合，線溶系の活性が極端に亢進し血液が流動性となるため，死後CT上，心大血管内腔の血液は高吸収水平面形成（図11）を示すことが多い[18]．線溶系活性亢進の原因は，1）死戦期から死後にかけて血中に種々の血管作動物質（カテコールアミン，ヒスタミンなど）が極端に増量し，それらが血管壁受容体を介して血管内皮よりプラスミノーゲンアクチベータを放出させる，2）死後のアシドーシスの進行程度がきわめて高度で，そのため血管内皮細胞膜の変性，崩壊も急激に進みプラスミノーゲンアクチベータの大量流出が起こる，とされている．死戦期が長い場合には，水平面を形成せずに，鋳型のような高吸収構造を示すことが多い[30]（図14）．

肺の荷重部陰影は，荷重部のうっ血と肺自身の重量による無気肺で生じるとされ，生きているヒトのCTでも出現する．死後CT上，血液就下は荷重部陰影を増強する[20]（図15）．

b. 右心系拡張

死後，両心系の圧は平均循環充満圧（全循環が停

A　死亡確認直後の腹部CT

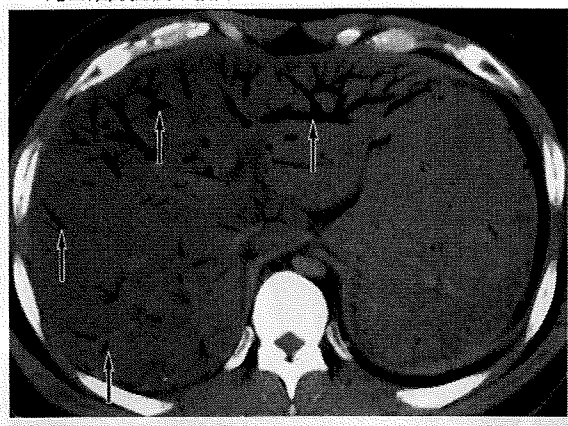

B　死亡後のvolume rendering像

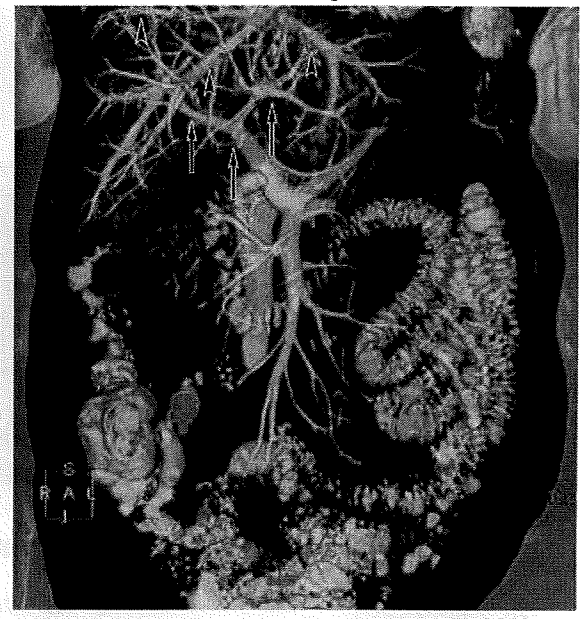

図13　門脈ガスと肝静脈ガス

A, B：腹部の死後CT(A)は，肝血管内ガスを示す(→)．このような死後CTの気体のみを描出したvolume rendering像(B)は，門脈ガス(→)と肝静脈ガス(►)の把握がしやすい．

(Bは千葉大学医学部附属病院Aiセンター 山本正二先生，下総良太先生のご厚意による)

死亡1日後の胸部CT

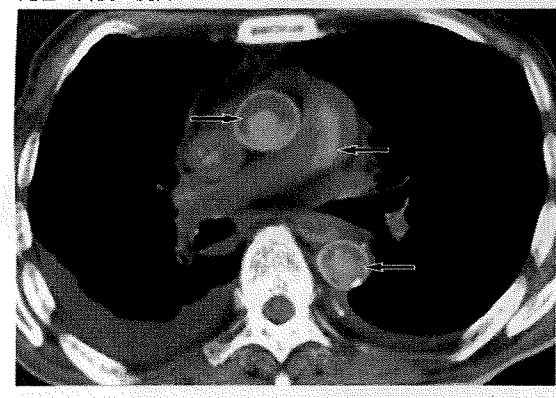

図14　水平面形成を示さない凝血塊

死後硬直が出現した状態で発見されたので心肺蘇生術を施行しなかった患者(死因は不詳)．死亡1日後のCTは，心大血管内腔に鋳型のような高吸収凝血塊(→)を示す．

死亡確認直後の胸部CT

図15　肺の血液就下

背側肺の吸収値上昇(→)を示す．

止した時に血管の各部が一様に示す静的な平衡圧)の約7mmHgに収束する[21]．この死後の血圧は血液量が多いとより高くなる．平均循環充満圧は，生前の右心系や左房の拡張圧より少し高いため，死後に右心系は拡張する[37]．例えば，生前の正常な上大静脈圧(中心静脈圧)は4～7mmHg(5～10cmH_2O)で，上大静脈はCT上の横断像で楕円形を示すことが多いが，死後には必ず円形となる(図16)．

c．動脈壁の高吸収化[38]

死後に血圧が平均循環充満圧まで低下すると，動脈の血管径は短縮し，血管壁は厚く，密度も高くなるため，死後CT上，血管壁の高吸収化が起こる．血管壁の高吸収化は，気管分岐部レベル(～その1cm尾側)の上行大動脈で最も典型的に認め，同部の平均直径は生前3.5cmから死後2.9cmへと短縮し，壁厚も2mmとなる．上行大動脈壁の高吸収化は，すべての死後CTで認める所見である(図16)．

A　生前の胸部CT

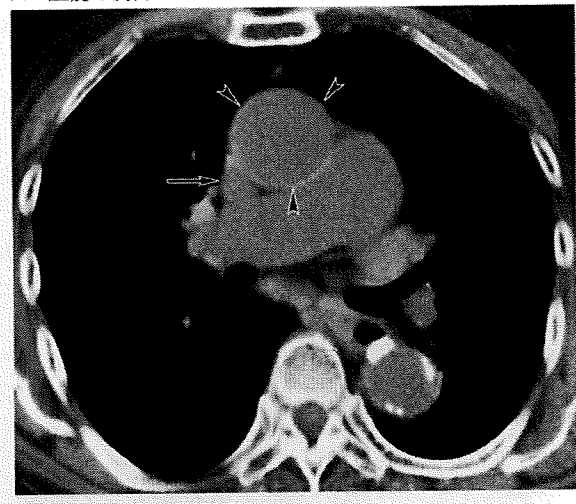

B　死亡確認直後の胸部CT

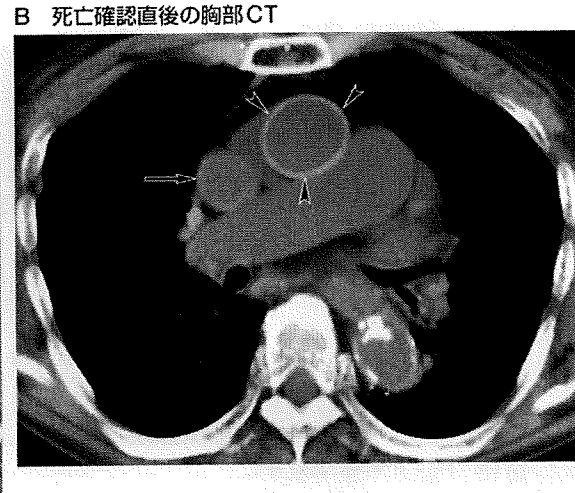

図16　右心系拡張と大動脈壁高吸収化
A, B：生前CT(A)と比較すると死後CT(B)は上大静脈拡張(→)と大動脈壁高吸収化(►)を示す.

A　死後の頭部CT

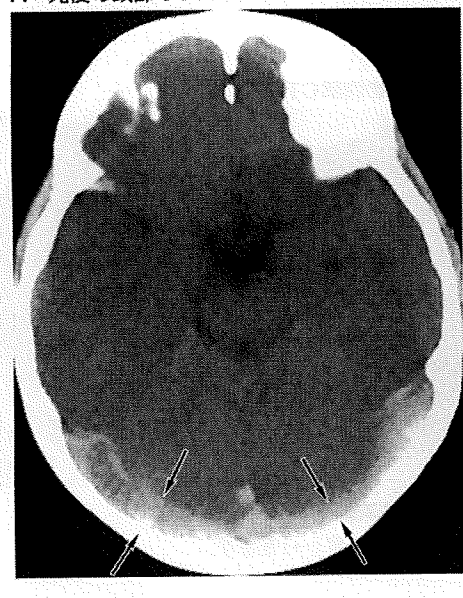

B　解剖

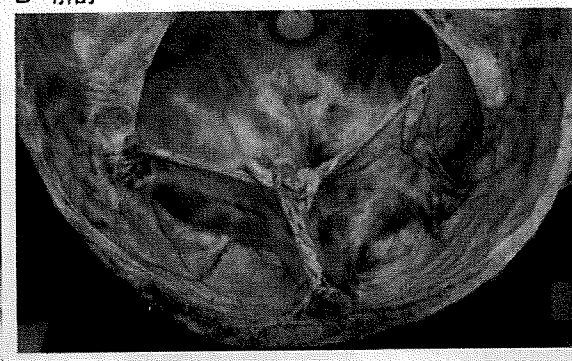

図17　静脈洞高吸収
A, B：死後CT(A：→)は静脈洞高吸収を示す．解剖(B)は硬膜下血腫を否定する.

2) 頭　部

a. 血液就下

生きているヒトのCT上，頭部の静脈洞(横静脈洞，S状静脈洞，上矢状静脈洞)は軽度高吸収を呈するが，死後CTでは血液就下が同所見を増強する[39] (図17)．これらは，硬膜下血腫と間違えやすい．

b. 脳浮腫

脳梗塞の超急性期(発生から1日以内)では細胞性浮腫，それ以降の急性期では細胞性浮腫と血管性浮腫が混在する．生きているヒトのCT上，超急性期脳梗塞の所見は，基底核の輪郭の不明瞭化，皮質と皮質下白質とのコントラスト低下，脳回の軽度腫脹による脳溝の不明瞭化である．死亡の直前・直後に撮影された死後CTは，超急性期の全脳虚血状態に相当し，脳実質は正常～軽度脳浮腫所見を示す(図18)．死後半日以上が経過したような死後CTでは，白質/灰白質のコントラスト低下と脳溝の不明瞭化は増強し，脳室と脳溝が狭小化すると報告されている[40]が，通常の脳梗塞のような低吸収にはならない．

A　死亡7時間前の頭部CT　　B　死亡7時間後の頭部CT

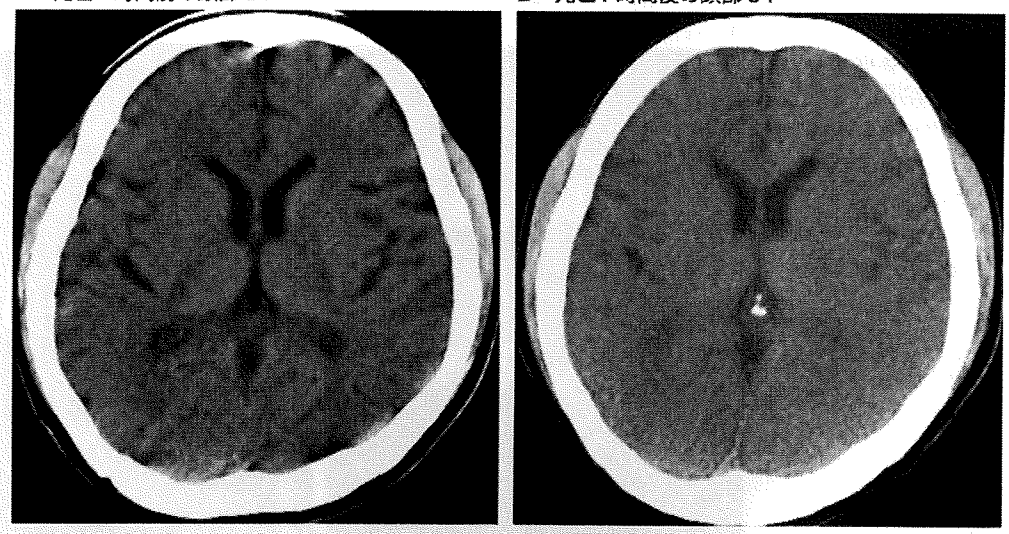

図18　脳浮腫

A，B：生前CT(A)と比較すると，死後CT(B)は白質/灰白質境界と脳溝の不明瞭化を示す．

A～C　死亡3日後のCT

A　頭部

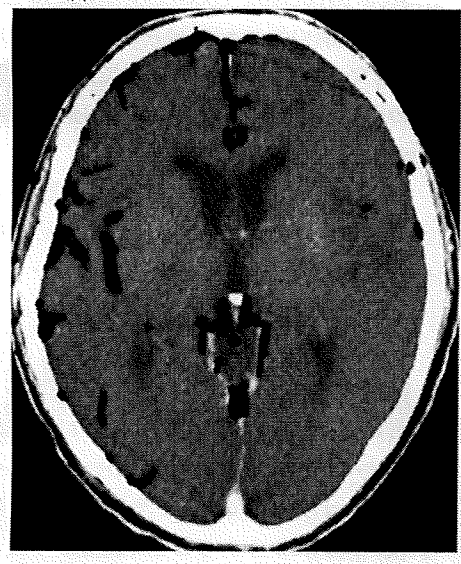

B　胸部

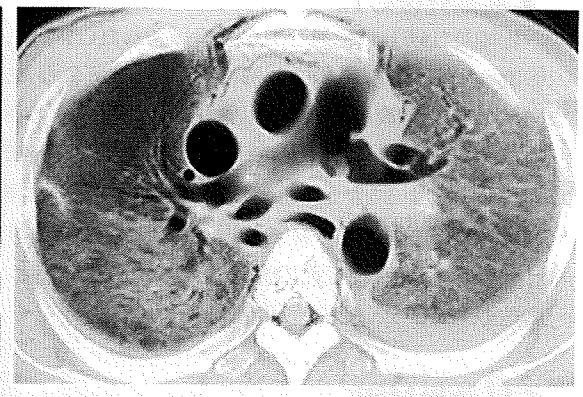

C　腹部

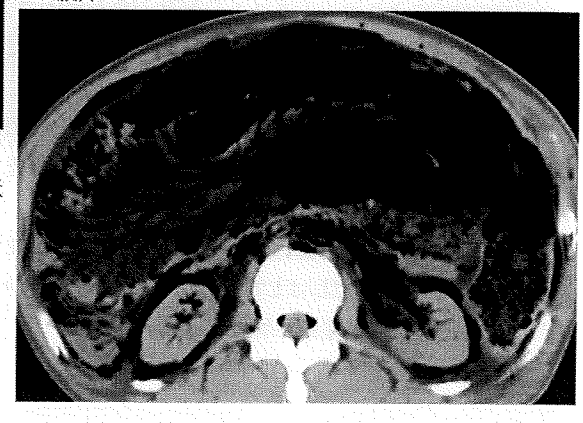

図19　腐敗

A～C：頭・胸・腹部の広範な血管内ガスを示す．

(推薦図書2)より転載)

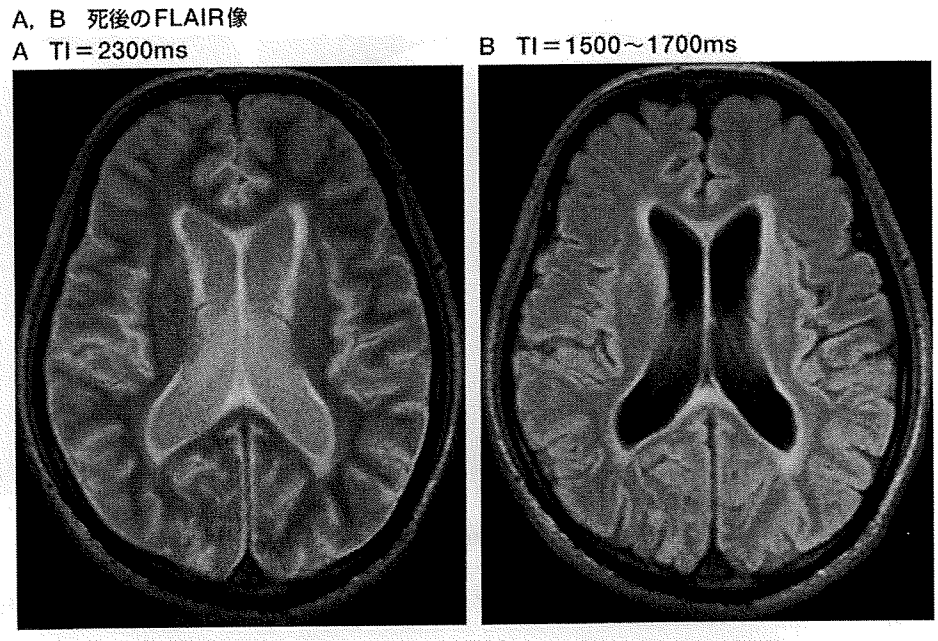

図20 cold FLAIR
A, B：脳脊髄液信号は，生体での撮像条件TI＝2300ms(A)では抑制されないが，TI＝1500～1700ms(B)で抑制される．

9. 晩期死後CT

死後半日以上が経過してから撮影されたCTでは，腐敗（細菌による死体の分解）が目立つようになる．腐敗の初期体表所見は，死後1日以降に出現する下腹部の緑色の変色（硫化ヘモグロビン，硫化メトヘモグロビンによる）だが，死後CTはそれより前の段階の腐敗を，血管内ガス粒～空虚な血管腔として示す（図19）．蘇生術後変化で血管内ガスが出現すると，腐敗の進行が早いと言う印象を持っている．

10. 死後MRI

MRIはCTよりコントラスト分解能が優れており，時間をかければ高分解能画像も撮像できる．これにより，CTでは評価困難な虚血心筋（図6），脳幹梗塞，頸髄損傷，肺動脈血栓塞栓症（図8），肝腫瘤や肝損傷などが検出でき，画像による死因確定率の上昇を期待できる．

死後MRIで得た信号や組織間コントラストは，生体におけるそれらとしばしば異なる．原因のひとつは低温（死後変化と冷蔵庫保存による）である[41][42]．例えば，生体と同じ条件で死体頭部のfluid attenuated inversion recovery(FLAIR)を撮像すると，脳脊髄液の信号が抑制されない（図20）．温度が低下するとT1値は短縮するので，温度の低い脳脊髄液の信号を抑制するためには，TI値を短縮させる必要がある．

生体に対するMRIの技術は，機能，代謝，血流に関するものを除いて，死後MRIに応用できる．高磁場MRI装置を用いたオートプシー・イメージング・システム開発の研究[43]も始まっている．

おわりに

死後画像上の所見をどのように解釈すればよいかを述べたが，所見の成因については我々の仮説が少なからず交じっている．多くの放射線科医が死後画像の読影にかかわることで間違いが訂正され，エビデンスとして確立されることを望んでいる．

謝 辞

三井住友海上福祉財団から研究助成を受けた．

本稿の要旨は，2009年ミッドサマーセミナー（日本放射線科専門医会・医会主催）のカレントトピックスおよび2009年日本医学放射線学会秋季臨床大会の教育講演で発表した．

■文献

1) 江澤英史: 死亡時医学検索におけるオートプシー・イメージングの重要性. 画像診断 25: 356-364, 2005.
2) 阪本奈美子, 大橋教良, 濱邊祐一・他: 全国救命救急センターにおける死後画像取得の現状と課題についてのアンケート調査結果報告. 救急医学 33: 985-989, 2009.
3) 日本医師会 死亡時画像病理診断（Ai＝Autopsy imaging）活用に関する検討委員会: 死亡時画像病理診断（Ai）の実態の把握及び今後の死亡時医学検索の具体的な展開の方途について. http://dl.med.or.jp/dl-med/teireikaiken/20090401_4.pdf
4) 白川洋一, 竿坂邦彦, 山下正人・他: 交通事故で急死した症例に対する死後全身CT撮影の意義. 日救急医会誌 7: 273-280, 1996.
5) 菅原俊祐, 水沼仁孝, 加藤弘毅・他: 死因推定におけるCT（Postmortem CT）の有用性. 臨床放射線 51: 845-850, 2006.
6) 音見暢一, 金只賢治, 向所敏文・他: 来院時心肺停止患者107例の死後CT撮影の検討. 臨床画像 24: 514-518, 2008.
7) 杉村 宏, 矢埜正美, 竹智義臣・他: 心肺停止症例の死因検索におけるCTの有用性. 救急医学 32: 861-864, 2008.
8) 高橋直也, 樋口健史, 塩谷 基・他: 死後CT（オートプシー・イメージング）360例における死後所見・心肺蘇生術後所見の検討. 臨床放射線 53: 1840-1845, 2008.
9) Shiotani S, Shiigai M, Ueno Y, et al: Postmortem computed tomography findings as evidence of traffic accident-related fatal injury. Radiat Med 26: 253-260, 2008.
10) Donchin Y, Rivkind AI, Bar-Ziv J, et al: Utility of postmortem computed tomography in trauma victims. J Trauma 37: 552-556, 1994.
11) Farkash U, Scope A, Lynn M, et al: Preliminary experience with postmortem computed tomography in military penetrating trauma. J Trauma 48: 303-308, 2000.
12) Aghayev E, Sonnenschein M, Jackowski C, et al: Postmortem radiology of fatal hemorrhage: measurements of cross-sectional areas of major blood vessels and volumes of aorta and spleen on MDCT and volumes of heart chambers on MRI. AJR 187: 209-215, 2006.
13) Hoey BA, Cipolla J, Grossman MD, et al: Postmortem computed tomography, "CATopsy", predicts cause of death in trauma patients. J Trauma 63: 209-215, 2007.
14) Sochor MR, Trowbridge MJ, Boscak A, et al: Postmortem computed tomography as an adjunct to autopsy for analyzing fatal motor vehicle crash injuries: results of a pilot study. J Trauma 65: 659-665, 2008.
15) Christe A, Ross S, Oesterhelweg L, et al: Abdominal trauma-sensitivity and specificity of postmortem noncontrast imaging findings compared with autopsy findings. J Trauma 66: 1302-1307, 2009.
16) Aghayev E, Thali MJ, Sonnenschein M, et al: Postmortem tissue sampling using computed tomography guidance. Forensic Sci Int 166: 199-203, 2007.
17) Weustink AC, Hunink MGM, van Dijke CF, et al: Minimally invasive autopsy: an alternative to conventional autopsy? Radiology 250: 897-904, 2009.
18) Shiotani S, Kohno M, Ohashi N, et al: Postmortem intravascular high density fluid level (Hypostasis): CT findings. J Comput Assist Tomogr 26: 892-893, 2002.
19) Shiotani S, Watanabe K, Kohno M, et al: Postmortem computed tomographic (PMCT) findings of pericardial effusion due to acute aortic dissection. Radiat Med 22: 405-407, 2004.
20) Shiotani S, Kohno M, Ohashi N, et al: Non-traumatic postmortem computed tomographic (PMCT) findings of the lung. Forensic Sci Int 139: 31-48, 2004.
21) Guyton AC, John EH: 心拍出量, 静脈還流, およびその調節. Guyton AC, John EH（編）; 早川弘一（監訳）; ガイトン臨床生理学. 第1版, 医学書院, p.241-253, 1999.
22) Jackowski C, Sonnenschein M, Thali MJ, et al: Virtopsy: postmortem minimally invasive angiography using cross section techniques-implementation and preliminary results. J Forensic Sci 50: 1175-1186, 2005.
23) Grabherr S, Djonov V, Yen K, et al: Postmortem angiography: review of former and current methods. AJR 188: 832-838, 2007.
24) Ross S, Spendlove D, Bolliger S, et al: Postmortem whole-body CT angiography: evaluation of two contrast media solutions. AJR 190: 1380-1389, 2008.
25) Persson A, Jackowski C, Engstrom E, et al: Advances of dual source, dual-energy imaging in postmortem CT. Eur J Radiol 68: 446-455, 2008.
26) 阪本奈美子, 菊野隆明: 14 急性大動脈解離（造影CT）. オートプシー・イメージング読影ガイド. 第1版, 文光堂, 2009.
27) 横田 元, 藤本 肇: 診療放射線技師のためのAi（Autopsy imaging）入門. 第7回 地方病院におけるAiの実際－沼津市立病院の取り組み. 日本放射線技師会誌 56: 993-997, 2009.
28) Jackowski C, Christe A, Sonnenschein M, et al: Postmortem unenhanced magnetic resonance imaging of myocardial infarction in correlation to histological infarction age characterization. Eur Heart J 27: 2459-2467, 2006.
29) Shiotani S, Yamazaki K, Kikuchi K, et al: Postmortem magnetic resonance imaging (PMMRI) demonstration of reversible injury phase myocardium in a case of sudden death from acute coronary plaque change. Radiat Med 23: 563-565, 2005.
30) Patriquin L, Kassarjian A, Barish M, et al: Postmortem whole-body magnetic resonance imaging as an adjunct to autopsy: preliminary clinical experience. J Magn Reson Imaging 13: 277-287, 2001.
31) Arai A, Shiotani S, Yamazaki K, et al: Postmortem computed tomographic (PMCT) and postmortem magnetic resonance imaging (PMMRI) demonstration of fatal massive retroperitoneal hemorrhage caused by abdominal aortic aneurysm (AAA) rupture. Radiat Med 24: 147-149, 2006.
32) Shiotani S, Kohno M, Ohashi N, et al: Cardiovascular gas on non-traumatic postmortem computed tomography (PMCT): the influence of cardiopulmonary resuscitation. Radiat Med 23: 225-229, 2005.
33) Shiotani S, et al: Non-traumatic postmortem computed tomographic demonstration of cerebral gas embolism following cardiopulmonary resuscitation. Jpn J Radiol (in press).
34) Shiotani S, Kohno M, Ohashi N, et al: Postmortem computed tomographic (PMCT) demonstration of the relation between gastrointestinal (GI) distension and hepatic portal venous gas (HPVG). Radiat Med 22: 25-29, 2004.
35) Jackowski C, Sonnenschein M, Thali MJ, et al:

Intrahepatic gas at postmortem computed tomography: forensic experience as a potential guide for *in vivo* trauma imaging. J Trauma 62: 979-988, 2007.
36) Takahashi N, Higuchi T, Shiotani M, et al: Intrahepatic gas at postmortem multislice computed tomography in cases of nontraumatic death. Jpn J Radiol 27: 264-268, 2009.
37) Shiotani S, Kohno M, Ohashi N, et al: Dilatation of the heart on postmortem computed tomography (PMCT): comparison with live CT. Radiat Med 21: 29-35, 2003.
38) Shiotani S, Kohno M, Ohashi N, et al: Hyperattenuating aortic wall on postmortem computed tomography (PMCT). Radiat Med 20: 201-206, 2002.
39) 小林雅彦, 渡辺 慎, 高田 綾・他: 頭部CTにて外傷性頭蓋内出血と診断され, 剖検で否定された乳児CPA症例. 救急医学 27: 617-619, 2003.
40) Sarwar M, McCormick WF: Decrease in ventricular and sulcal size after death. Radiology 127: 409-411, 1978.
41) 塩谷清司, 齋藤 創, 糸屋沙央梨・他: 診療放射線技師のためのAi (Autopsy imaging) 入門. 第4回 死後画像所見. 日本放射線技師会誌 56: 459-469, 2009.
42) Kobayashi T, Shiotani S, Kaga K, et al: Characteristic signal intensity changes on postmortem magnetic resonance imaging of the brain. Jpn J Radiol (in press).
43) 文部科学省ホームページ: 平成21年度科学研究費補助金 (新学術領域研究) 採択研究領域及び採択研究課題一覧 http://www.mext.go.jp/a_menu/shinkou/hojyo/1281894.htm

■推薦図書

1) 江澤英史, 塩谷清司 (編著): オートプシー・イメージング－画像解剖. 第1版, 文光堂, 2004.
2) 大友 邦 (監修): 塩谷清司, 山本正二 (編): オートプシー・イメージング読影ガイド. 第1版, 文光堂, 2009.
3) 日本放射線科専門医会・医会A: ワーキンググループ, 社団法人 日本放射線技師会A: 活用検討委員会 (編): オートプシー・イメージングガイドライン. 第1版, ベクトルコアー, 2009.
4) Brogdon BG (編): Forensic Radiology. 第1版, CBC Press, 1998.
5) Thali MJ, Dirnhofer R, Vock P (編): The VIRTOPSY APPROACH. 第1版, CBC Press, 2009.
[内容を手っ取り早く知りたい方は, 'Dirnhofer R, Jackowski C, Vock P, et al: VIRTOPSY: minimally invasive, imaging-guided virtual autopsy. Radiographics 26: 1305-1333, 2006.' を参照]

Summary

Autopsy imaging (Ai): Postmortem Imaging Findings

Seiji Shiotani*, Hideyuki Hayakawa**, Kazunori Kikuchi***, et al

Among postmortem imaging, radiologists are most frequently asked to interpret CT performed immediately before or after death in patients carried into an emergency room in a state of cardiopulmonary arrest on arrival. Postmortem CT findings are classified into three categories: (1) causes of death (traumatic/non-traumatic), (2) changes occurred due to cardiopulmonary resuscitation, and (3) postmortem changes. Traumatic causes of death can be identified by CT at high rate. In non-traumatic deaths, hemorrhagic causes of death can be identified. Knowledge regarding typical postmortem CT findings of (2) and (3) is important when diagnosing non-traumatic deaths.

*Department of Radiology, Tsukuba Medical Center, **Department of Forensic Medicine, Tsukuba Medical Examiner's Office, ***Department of Pathology, Tsukuba Medical Center

Jpn J Radiol (2010) 28:1–7
DOI 10.1007/s11604-009-0372-x

ORIGINAL ARTICLE

Nontraumatic postmortem computed tomographic demonstration of cerebral gas embolism following cardiopulmonary resuscitation

Seiji Shiotani · Yukihiro Ueno · Shigeru Atake
Mototsugu Kohno · Masatsune Suzuki
Kazunori Kikuchi · Hideyuki Hayakawa

Received: May 10, 2009 / Accepted: August 26, 2009

Abstract
Purpose. The aim of this study was to investigate cerebral gas embolism (GE) on nontraumatic postmortem CT (PMCT), regarding its frequency, location (arterial or venous), and causes.
Materials and methods. Our subjects were 404 nontraumatically deceased patients who had been in a state of cardiopulmonary arrest on arrival at our emergency room. PMCT was performed within 2 h of the confirmation of death.
Results. Cardiopulmonary resuscitation (CPR) was performed on 387 of the 404 subjects; and of these, cerebral GE was detected in 29 (7.5%) subjects (3 arterial, 25 venous, 1 undeterminable). Cerebral GE was not noted in the other 17 of the 404 subjects who did not undergo CPR. However, there was no significant difference in the incidence of cerebral GE between the subjects who underwent CPR and those who did not. The mechanism of cerebral arterial GE was presumed due to pulmonary barotrauma and/or paradoxical embolism, while the thoracic pump theory was suggested to explain the cerebral venous GE.
Conclusion. Cerebral arterial/venous GE is found in CPR cases on nontraumatic PMCT.

Key words Postmortem computed tomography · Cerebral gas embolism · Cardiopulmonary resuscitation

S. Shiotani (✉)
Department of Radiology, Tsukuba Medical Center,
1-3-1 Amakubo, Tsukuba 305-8558, Japan
Tel. +81-29-851-3511; Fax +81-29-858-2773
e-mail: shiotani@tmch.or.jp

Y. Ueno · S. Atake · M. Kohno
Department of Critical Care and Emergency Medicine, Tsukuba Medical Center, Tsukuba, Japan

M. Suzuki
Department of General Internal Medicine, Tsukuba Medical Center, Tsukuba, Japan

K. Kikuchi
Department of Pathology, Tsukuba Medical Center, Tsukuba, Japan

H. Hayakawa
Department of Forensic Medicine, Tsukuba Medical Examiner's Office, Tsukuba, Japan

This article was presented at the Japan Radiology Congress, Yokohama, April 2008

Introduction

In light of the number of autopsies currently being performed, postmortem examination using imaging modalities such as computed tomography (CT), magnetic resonance imaging (MRI), ultrasonography, and angiography has been proposed as an alternative to or a concomitant method for autopsy.[1–13] In Japan, as the medical examiner system does not extend nationwide, about 80% of major facilities with emergency rooms (ERs) use postmortem CT (PMCT) to detect the cause of death in patients arriving at the ER in a state of cardiopulmonary arrest (CPA).[14–18] As the need for and frequency of PMCT increase worldwide for the purpose of determining the cause of death, diagnostic methods that aid the interpretation of PMCT findings such as intravascular gas in the heart, great vessels, and liver need to be established.[19,20]

Cerebral gas embolism (GE) is thought to occur accidentally,[21–23] iatrogenically,[24,25] and as a result of cardio-

pulmonary resuscitation (CPR) after CPA.[26–35] On PMCT imaged immediately before or after death in traumatically deceased cases, only arterial findings of cerebral GE due to CPR have been reported.[27–33] In contrast, both arterial and venous GE findings have been reported in nontraumatically deceased cases.[26,27,34,35] Any analysis of cerebral GE induced by CPR should exclude the possible effects of trauma. However, the published literature on the subject is limited, and the nature of GE remains unclear with regard to its frequency of occurrence and whether it occurs more commonly in arteries or veins. In this study, we investigated cerebral GE on PMCT in nontraumatically deceased subjects and discussed its possible mechanisms.

Materials and methods

Our subjects were 404 nontraumatically deceased patients for whom death was confirmed after arriving at our ER in a state of CPA between January 2000 and December 2007. They included 274 men and 130 women, ranging in age from 0 to 101 years (mean 67 years). CPR was performed on 387 of the 404 subjects during transport and in our ER by artificial respiration with bag-valve masking and intratracheal intubation, continuous chest compression, and infusion. CPR was not performed on 17 of the 404 subjects because they had already exhibited early signs of death (postmortem hypostasis is usually apparent within 30 min to 2 h following death, as is rigor mortis at about 4 h after death), although there was no indication of putrefaction.

Causes of death were diagnosed based on a comprehensive understanding of the patient's present illness, clinical history, and PMCT findings. A fatal hemorrhagic lesion was defined when PMCT detected a subarachnoid hemorrhage, cerebral hemorrhage, aortic dissection, or rupture of abdominal aortic aneurysm. For diagnosis of acute heart failure, a frequent cause of death, PMCT cannot detect direct findings, such as thromboembolism of the coronary artery or ischemic myocardium.[36] Therefore, we diagnosed acute heart failure when pulmonary edema was seen on PMCT, which is an indirect finding that results from cardiac pump failure.[37] Autopsy findings were also obtained in 29 cases for which we were able to secure family consent.

PMCT was performed within 2 h of the confirmation of death in the Radiology Department of our institution with the prior approval of the institutional review board. Two clinical CT scanners were used for PMCT. Until April 2004, PMCT was performed with a single-detector CT scanner (Accel Proceed; GE-Yokogawa Medical Systems, Tokyo, Japan) in conventional scan mode without using the helical scan technique. The scan parameters for the head were as follows: 120 kV, 160 mA, 2.0 s/rotation, contiguous 5-mm sections from the orbitomeatal line to the pentagon level, and 10-mm sections in the upper area. The scan parameters for the thorax, abdomen, and pelvis were 120 kV, 250 mA, 1.0 s/rotation, and 15-mm intervals with 10 mm collimation. A neck CT scan was omitted because the attending emergency physician, who performed CPR on the patient, thought that the cervical spine was not injured based on a comprehensive understanding of the patient's present illness, clinical history, and physical examination; thus, the cause was categorized as a nontraumatic death.

From April 2004, PMCT was performed with a 16-channel multidetector row CT (MDCT) scanner (Aquilion 16; Toshiba Medical Systems, Tokyo, Japan). The scan parameters for the head were conventional scan mode 120 kV, 200 mA, 2.0 s/rotation, 1 mm collimation, and contiguous 4-mm sections. The scan parameters for the thorax, abdomen, and pelvis were helical scan mode, 120 kV, 300 mA, 0.7 s/rotation, 1 mm collimation, pitch 15, and contiguous 10-mm sections. The neck region was not scanned for the same reason as described above. All images were observed on a 21-inch monochrome monitor with 1600 × 1200 pixels at appropriate window settings for each region.

A board-certified radiologist and board-certified emergency medicine physicians retrospectively reviewed PMCT findings of the brain, thorax, abdomen, and pelvis. We determined whether cerebral GE was present by means of consensus. Cerebral arterial GE[26–33] was defined as when one or more of the following arteries contained gas: the internal carotid artery (cavernous and supraclinoid segments) or the anterior, middle, or posterior cerebral artery. Cerebral venous GE[34,35,38,39] was defined as when the posterior cranial fossa or venous sinuses contained gas. Cardiovascular gas and other abnormal findings associated with cerebral GE were also recorded if present.

The chi-squared test for independence was used to determine whether differences between the incidence of cerebral GE in patients who received CPR and that in those who did not were statistically significant. A two-tailed probability value of $P < 0.05$ was considered statistically significant.

Results

Cerebral GE was detected in 29 (7.5%) of the 387 subjects who underwent CPR. No cerebral GE was detected in the 17 subjects who did not receive CPR. The differ-

ence between the two groups was not statistically significant ($\chi^2 = 1.35 < 3.84 = \chi^2_{0.05}$).

Arterial GE was detected in 3 of the 29 cerebral GE subjects: an 11-day-old male baby (case 1: cause of death acute circulatory failure); a 1 month-old female baby (cause of death: congestive heart failure and pneumonia), and a 2 month-old male baby (cause of death: pneumonia). PMCT of the thorax showed cardiovascular gas in the right atrium and bilateral ventricles in all three subjects. Autopsies performed on the 11-day old male infant and the 1 month-old female infant confirmed the presence of a right-to left-shunt. Also, the autopsies in these two cases revealed gas bubbles in the leptomeningeal vessels and in the bilateral anterior, middle, and posterior cerebral arteries. Autopsy was not performed on the 2-month-old male infant for whom the cause of death was diagnosed as pneumonia because of his signs and symptoms, including leukocytosis and extensively increased attenuation in the lung on PMCT.

Venous GE was detected in 25 of the 29 cerebral GE subjects. The causes of death of these 25 subjects were acute heart failure (17 subjects), pneumonia (3), aortic dissection (2), cerebral hemorrhage (1), suicide by ingesting hypnotic drugs (1), and choking on food (1). These 25 subjects showed either a spotty or linear-shaped venous GE in the cerebellum (case 2); one subject also showed GE in the cavernous sinus. PMCT of the thorax in 23 of these 25 subjects showed vascular gas in at least one of three veins: jugular, subclavian, and brachiocephalic. Autopsy was performed on a 37-year-old woman (who committed suicide by excessive ingestion of hypnotic drugs) and a 40-year-old man (who had acute heart failure). The autopsies in these two cases were not able to identify the gas bubbles that were shown on PMCT.

Cerebral GE was detected along the surface of the left temporal lobe in 1 of the 29 subjects, but the location of the gas could not be specified as either arterial or venous (case 3).

Three typical cases are described.

Case descriptions

Case 1

An 11-day-old neonate was found not breathing in the morning. He had been diagnosed as having a heart murmur at birth. After being transferred to our ER by ambulance in a CPA state, he did not respond to CPR, and death was confirmed 60 min after arrival. To determine the cause of death, PMCT was performed. PMCT of the brain showed arterial GE (Fig. 1a). PMCT of the thorax showed cardiovascular gas in the right atrium, bilateral ventricles, and ascending aorta (Fig. 1b). Autopsy revealed multiple heart anomalies (atrial septal defect, ventricular septal defect, patent ductus arteriosus) and severe pulmonary edema. Autopsy also revealed gas bubbles in the leptomeningeal vessels and in the bilateral anterior, middle, and posterior cerebral arteries. The cause of death was diagnosed as acute circulatory failure.

Case 2

An 81-year-old woman was found unconscious. She had been undergoing dialysis for the previous 3 months. After being transferred to our ER by ambulance in a CPA state, she did not respond to CPR, and death was confirmed 30 min after arrival. Although no autopsy was performed, the cause of death was diagnosed as acute heart failure based on her medical history and clinical course. PMCT was performed to exclude definitively other possible causes. PMCT of the brain showed venous GE (Fig. 2a). PMCT of the thorax showed cardiovascular gas in the left brachiocephalic vein (Fig. 2b).

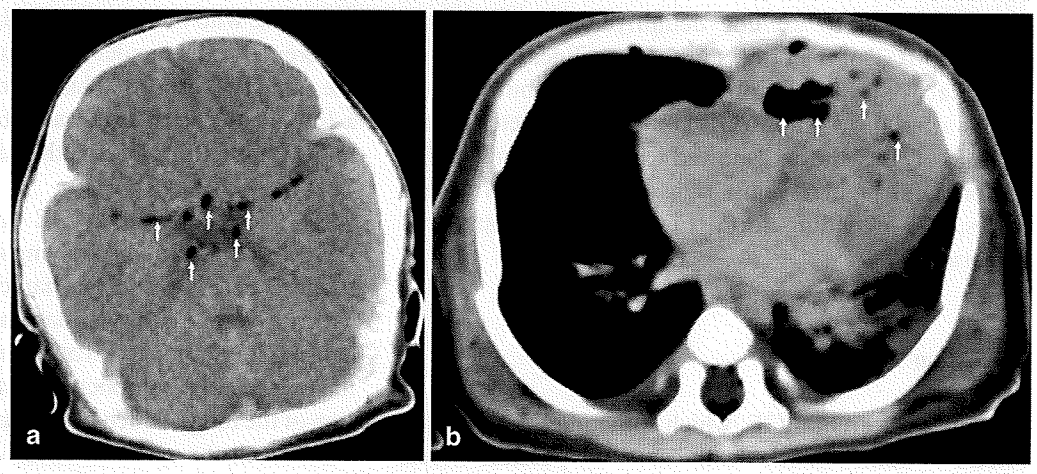

Fig. 1. **a** Postmortem computed tomography (PMCT) of the brain shows gas bubbles in the proximal parts of the bilateral anterior, middle, and posterior cerebral arteries (*arrows*). **b** PMCT of the thorax shows gas bubbles or retention in bilateral ventricles (*arrows*)

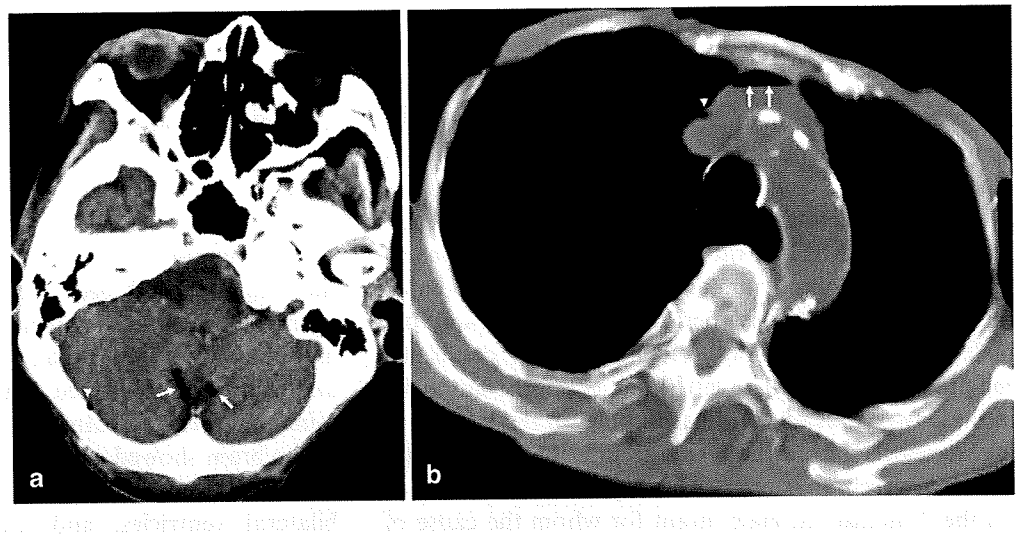

Fig. 2. **a** PMCT of the brain shows linear-shaped gas in the dorsal cerebellar vermis (*arrows*) and spotty gas along the surface of the right cerebellar hemisphere (*arrowhead*). **b** PMCT of the thorax shows a thin gas layer in the left brachiocephalic vein (*arrows*) and spotty gas in the superior vena cava (*arrowhead*)

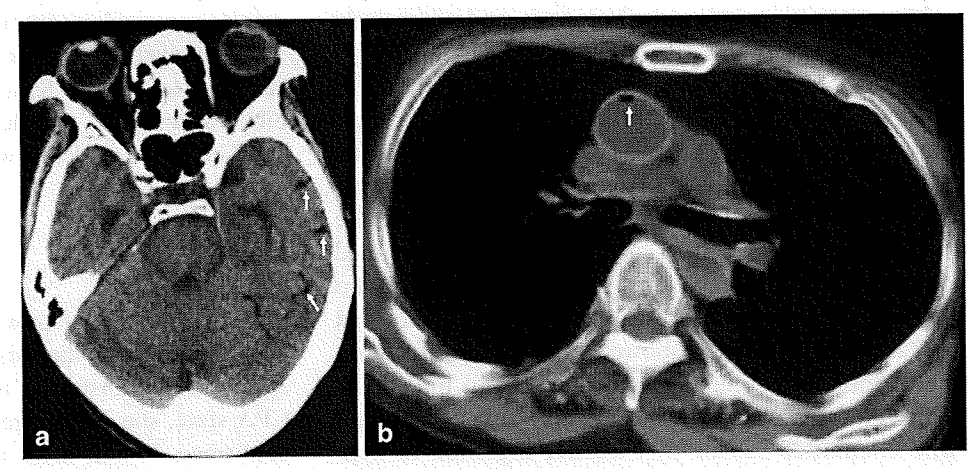

Fig. 3. **a** PMCT of the brain shows curvilinear gas along the surface of the left temporal lobe (*arrows*). **b** PMCT of the thorax shows spotty gas in the ascending aorta (*arrow*)

Case 3

An 84-year-old woman committed suicide by ingesting hypnotic drugs. After being transferred to our ER by ambulance in a CPA state, she did not respond to CPR, and death was confirmed 30 min after arrival. PMCT was performed to exclude definitively other possible causes. PMCT of the brain showed curvilinear GE along the surface of the left temporal lobe (Fig. 3a), but whether it was arterial or venous GE could not be determined. PMCT of the thorax showed cardiovascular gas in the bilateral jugular veins, right atrium, bilateral ventricles, and ascending aorta (Fig. 3b). No autopsy was performed.

Discussion

As causes of cerebral GE, which sometimes is shown by PMCT in nontraumatic death cases, the possible effects of CPR or putrefaction must be taken into consideration. In our study, the possibility of putrefaction was negated because PMCT was performed within 2 h of the confirmation of death. However, we found no statistically significant difference regarding the incidence of cerebral GE between the patients who underwent CPR and those who did not, although we did find a significant difference in the incidence of cardiovascular gas between the same two groups. This discrepancy is attributable to a low incidence of cerebral GE (7.5%) in subjects who underwent CPR, whereas that of cardiovascular gas was 71%.[19]

The cerebral arterial GE detected by nontraumatic PMCT of ER patients arriving in a CPA state is believed to be caused by the mechanical forces of CPR, such as positive-pressure ventilation and chest compression causing pulmonary barotrauma (rupturing of pulmonary vessels in conjunction with parenchymal destruction of the lung), which permits air to enter the pulmonary vein, reach the systemic circulation, and thus the intra-

cerebral arteries.[26–33] In our study, three subjects with cerebral arterial GE were pediatric cases. Arterial GE in pediatric cases can be theoretically explained as paradoxical embolism.[40] In contrast, in a study on nontraumatic PMCT, cardiovascular gas was seen in the right atrium of 36% of the subjects who underwent CPR and in the right ventricle in 41% of subjects,[19] suggesting that the gas was transported into the systemic circulation through the left atrium and ventricle by way of a right-to-left shunt such as an atrial and/or a ventricular septal defect.

Cerebral venous GE on nontraumatic PMCT can be explained by the thoracic pump theory.[34] In a study of nontraumatic PMCT, cardiovascular gas was detected in the brachiocephalic vein and superior vena cava of 45% of patients who underwent CPR.[19] The gas bubbles entering these veins are able to ascend retrogradely to the brain against the blood flow.[41] In patients for whom CPR is unsuccessful, antegrade venous flow does not occur and the gas is not carried away from the intracranial veins.

Rubinstein, et al.[38,39] reported that the distribution of cerebral GE varied among living individuals, and the causes were thought to include the time between the manipulation of intravenous lines and the CT scans, and the anatomy and position of the patient. In our study, venous GE was seen in the infratentorial region in all subjects; that is, its distribution was limited. We attributed this to the fact that the timing of PMCT was relatively constant, being within 2 h after confirmation of death, with the body remaining motionless in a supine position. Also, the diameter of the vessel is greatest from the sigmoid sinus to the transverse sinus, in the passageway from the internal jugular vein to the veins of the head.[42]

In two subjects who showed cerebral arterial GE on PMCT and who underwent an autopsy, gas bubbles in the vessels of the brain were found by autopsy, and the amount of gas was more than that shown on PMCT. Gas bubbles in the vessels of the brain are often detected at autopsy as an artifact. The causes include removal of the roof of the skull, which tears the meninges,[21] and dissection of the vessels near the medula oblongata to remove the brain from the skull. Postmortem imaging using CT or MRI is superior to autopsy for detecting gas in blood vessels and potential body cavities without altering the distribution of the gas.[43,44]

Nontraumatic PMCT findings are classified into three categories: (1) cause of death (e.g., subarachnoid hemorrhage and neurogenic pulmonary edema,[37] aortic dissection, cardiac tamponade[45]); (2) postmortem changes (e.g., hypostasis,[46] hyperattenuating aortic wall,[47] dilatation of the right heart[48]); and (3) changes that occur after CPR (e.g., cardiovascular gas,[19] gastrointestinal distention, hepatic portal venous gas[20]). In general, cerebral GE can be fatal; however, in our subjects, cerebral GE did not appear to be a direct cause of death. Autopsy was performed on two of three pediatric subjects who had arterial GE, and the cause of death was determined in each case (acute circulatory failure, congestive heart failure, and pneumonia). In the other subject who did not undergo autopsy, the cause of death was diagnosed as pneumonia based on a comprehensive understanding of the patient's present illness, blood count, and PMCT findings. Although 25 subjects showed a small amount of venous GE, such a small amount of GE is considered asymptomatic even in living individuals.[38,39]

The present study lacked neck region scans. Therefore, we could not define the relation between cerebral GE and vascular gas in the jugular vein. In a future study, we are planning to scan the neck regions of nontraumatically deceased patients using PMCT.

Conclusion

Cerebral arterial/venous GE was found in subjects who underwent CPR. Our study showed cerebral GE on PMCT in 29 subjects (7.5%), with venous GE more frequent than arterial GE. Furthermore, as the cause of the arterial GE observed in our pediatric cases, we suggest that cardiovascular gas caused by CPR had been transported into the systemic circulation by way of a right-to-left shunt.

Acknowledgments. This work was supported by a grant of the Public Trust-Foundation of Marumo ER Medicine & Research Institute. We thank Ms. Yumiko Moriyama for her help in manuscript preparation.

References

1. Brogdon BG. Research and applications of the new modalities. In: Brogdon BG, editor. Forensic radiology. 1st edn. Boca Raton: CRC Press; 1998. p. 333–8.
2. Swift B, Rutty GN. Recent advances in postmortem forensic radiology: computed tomography and magnetic resonance imaging applications. In: Tsokos M, editor. Forensic pathology reviews. 1st edn. Totowa: Humana; 2006. p. 355–404.
3. Uchigasaki S. Postmortem ultrasound imaging in forensic pathology. In: Tsokos M, editor. Forensic pathology reviews. 1st edn. Totowa: Humana; 2006 p. 405–12.
4. Dirnhofer R, Jackowski C, Vock P, Potter K, Thali MJ. Virtopsy: minimally invasive, imaging-guided virtual autopsy. Radiographics 2006;26:1305–33.
5. Hayakawa M, Yamamoto S, Motani H, Yajima D, Sato Y, Iwase H. Does imaging technology overcome problems of conventional postmortem examination? A trial of computed

tomography imaging for postmortem examination. Int J Legal Med 2006;120:24–6.
6. Oyake Y, Aoki T, Shiotani S, Kohno M, Ohashi N, Akutsu H, et al. Postmortem computed tomography for detecting causes of sudden death in infants and children: retrospective review of cases. Radiat Med 2006;24:493–502.
7. Chew FS, Relyea-Chew A, Ochoa ER Jr. Postmortem computed tomography of cadavers embalmed for use in teaching gross anatomy. J Comput Assist Tomogr 2006;30:949–54.
8. Ljung P, Winskog C, Persson A, Lundstrom C, Ynnerman A. Full body virtual autopsies using a state-of-the-art volume rendering pipeline. IEEE Trans Vis Comput Graph 2006;12: 869–76.
9. Poulsen K, Simonsen J. Computed tomography as routine in connection with medico-legal autopsies. Forensic Sci Int 2007;171:190–7.
10. Levy AD, Harcke HT, Getz JM, Mallak CT, Caruso JL, Pearse L, et al. Virtual autopsy: two- and three-dimensional multidetector CT findings in drowning with autopsy comparison. Radiology 2007;243:862–8.
11. O'Donnell C, Rotman A, Collett S, Woodford N. Current status of routine post-mortem CT in Melbourne, Australia. Forensic Sci Med Pathol 2008;3:226–32.
12. Shiotani S, Shiigai M, Ueno Y, Sakamoto N, Atake S, Kohno M, et al. Postmortem computed tomography findings as evidence of traffic accident-related fatal injury. Radiat Med 2008;26:253–60.
13. Weustink AC, Hunink MGM, van Dijke CF, Renken NS, Krestin GP, Oosterhuis JW. Minimally invasive autopsy: an alternative to conventional autopsy? Radiology 2009;250: 897–904.
14. Sakamoto N, Ohashi N, Hamabe Y, Kohno M, Shiotani S, Hayakawa H, et al. Answers to questionnaire regarding current status and future subjects of postmortem imaging in Japanese emergency center hospitals. Kyukyuigaku (Japanese Journal of Acute Medicine) 2009;33:985–9 (in Japanese).
15. Sugawara S, Mizunuma K, Kato K, Toshiyasu T. Evaluation of postmortem CT (PMCT) to diagnose the cause of death. Rinsho Hoshasen (Japanese Journal of Clinical Radiology) 2006;5:845–50 (in Japanese with English abstract).
16. Otomi Y, Kanetada K, Mukaijo T, Kourai F. Clinical experience of CT scannings to 107 postmortem examinations of CPAOA cases. Rinshogazou (Clinical Imagiology) 2008;24: 514–8 (in Japanese).
17. Sugimura H, Yano M, Takechi Y, Kawasaki Y, Tanaka T, Muranaka T, et al. Usefulness of postmortem computed tomography to investigate the cause of death in 135 cases of cardiopulmonary arrest on arrival. Kyukyuigaku (Japanese Journal of Acute Medicine) 2008;32:861–4 (in Japanese).
18. Takahashi N, Higuchi T, Shiotani M, Maeda H, Hirose Y, Iinuma Y, et al. Postmortem computed tomography in 360 deceased individuals: postmortem findings and influence of cardiopulmonary resuscitation. Rinsho Hoshasen (Japanese Journal of Clinical Radiology) 2008;53:1840–5 (in Japanese with English abstract).
19. Shiotani S, Kohno M, Ohashi N, Atake S, Yamazaki K, Nakayama H, et al. Cardiovascular gas on non-traumatic postmortem computed tomography (PMCT): the influence of cardiopulmonary resuscitation. Radiat Med 2005;23:225–9.
20. Shiotani S, Kohno M, Ohashi N, Yamazaki K, Nakayama H, Watanabe K. Postmortem computed tomographic (PMCT) demonstration of the relation between gastrointestinal (GI) distension and hepatic portal venous gas (HPVG). Radiat Med 2004;22:25–9.
21. Krants P, Holtas S. Postmortem computed tomography in a diving fatality. J Comput Assist Tomogr 1983;7:132–4.
22. Haydon JR, Williamson JA, Ansford AJ, Sherif S, Shapter MJ. A scuba-diving fatality. Med J Aust 1985;143:458–62.
23. Ozdoba C, Weis J, Platter T, Dirnhofer R, Yen K. Fatal scuba diving incident with massive gas embolism in cerebral and spinal arteries. Neuroradiology 2005;47:411–6.
24. Jensen ME, Lipper MH. CT in iatrogenic cerebral air embolism. AJNR Am J Neuroradiol 1986;7:823–7.
25. Kodama F, Ogawa T, Hashimoto M, Tanabe Y, Suto Y, Kato T. Fatal air embolism as a complication of CT-guided needle biopsy of the lung. J Comput Assist Tomogr 1999;23: 949–51.
26. Yamaki T, Ando S, Ohta K, Kubota T, Kawasaki K, Hirama M. CT demonstration of massive cerebral air embolism from pulmonary barotraumas due to cardiopulmonary resuscitation. J Comput Assist Tomogr 1989;13:313–5.
27. Shiina G, Shimosegawa Y, Kameyama M, Onuma T. Massive cerebral air embolism following cardiopulmonary resuscitation: report of two cases. Acta Neurochir (Wien) 1993;125: 181–3.
28. Iwama T, Andoh H, Murase S, Miwa Y, Ohkuma A. Diffuse cerebral air embolism following trauma: striking postmortem CT findings. Neuroradiology 1994;36:33–4.
29. Hashimoto Y, Yamaki T, Sakakibara T, Matsui J, Matui M. Cerebral air embolism caused by cardiopulmonary resuscitation after cardiopulmonary arrest on arrival. J Trauma 2000; 48:975–7.
30. Akaishi K, Hongo K, Obinata C, Kobayashi S. Pneumoangiogram in a patient with severe head injury: case illustration. J Neurosurg 2000;92:502.
31. Sakai I, Nishizawa S. Cerebral air embolism after lung contusion: case illustration. J Neurosurg 2001;95:909.
32. Ugurel S, Kocaoglu M, Saglam M, Ucoz T, Somuncu I. CT pneumoangiogram sign following cardiopulmonary resuscitation: detrimental cerebral air embolism or postmortem blood replacement with air? Eur J Radiol Extra 2003;45:114–7.
33. Hwang SL, Lieu AS, Lin CL, Liu GC, Howng SL, Kuo TH. Massive cerebral air embolism after cardiopulmonary resuscitation. J Clin Neurosci 2005;12:468–9.
34. Imanishi M, Nishimura A, Tabuse H, Miyamoto S, Sakaki T, Iwasaki S. Intracranial gas on CT after cardiopulmonary resuscitation: 4 cases. Neuroradiology 1998;40:154–7.
35. Sharma MR, Newell DW, Grant GA. Diffuse cerebral venous air embolism following subarachnoid hemorrhage: case illustration. J Neurosurg 2003;98:1320.
36. Shiotani S, Yamazaki K, Kikuchi K, Nagata C, Morimoto T, Noguchi Y, et al. Postmortem magnetic resonance imaging (PMMRI) demonstration of reversible injury phase myocardium in a case of sudden death from acute coronary plaque change. Radiat Med 2005;23:563–5.
37. Shiotani S, Kohno M, Ohashi N, Yamazaki K, Nakayama H, Watanabe K, et al. Non-traumatic postmortem computed tomographic (PMCT) findings of the lung. Forensic Sci Int 2004;139:39–48.
38. Rubinstein D, Symonds D. Gas in the cavernous sinus. Am J Neuroradiol 1994;15:561–6.
39. Rubinstein D, Dangleis K, Damiano TR. Venous air emboli identified on head and neck CT scans. J Comput Assist Tomogr 1996;20:559–62.
40. Muth CM, Shank ES. Gas embolism. N Engl J Med 2000;342: 476–82.
41. Schlimp CJ, Loimer T, Rieger M, Lederer W, Schmidts MB. The potential of venous air embolism ascending retrograde to the brain. J Forensic Sci 2005;50:906–9.
42. Pernkopf E. The head. In: Ferner H, editor. Atlas of topographical and applied human anatomy. 2nd revised edn. Munich: Urban & Schwarzenberg; Baltimore; 1980. p. 1–135.

43. Ros PR, Li KC, Vo P, Baer H, Staab EV. Preautopsy magnetic resonance imaging: initial experience. Magn Reson Imaging 1990;8:303–8.
44. Donchin Y, Rivkind AI, Bar-Ziv J, Hiss J, Almong J, Drescher M. Utility of postmortem computed tomography in trauma victims. J Trauma 1994;37:552–6.
45. Shiotani S, Watanabe K, Kohno M, Ohashi N, Yamazaki K, Nakayama H. Postmortem computed tomographic (PMCT) findings of pericardial effusion due to acute aortic dissection. Radiat Med 2004;22:405–7.
46. Shiotani S, Kohno M, Ohashi N, Yamazaki K, Itai Y. Postmortem intravascular high density fluid level (hypostasis): CT findings. J Comput Assist Tomogr 2002;26:892–3.
47. Shiotani S, Kohno M, Ohashi N, Yamazaki K, Nakayama H, Ito Y, et al. Hyperattenuating aortic wall on postmortem computed tomography (PMCT). Radiat Med 2002;20:201–6.
48. Shiotani S, Kohno M, Ohashi N, Yamazaki K, Nakayama H, Watanabe K, et al. Dilatation of the heart on postmortem computed tomography (PMCT): comparison with live CT. Radiat Med 2003;21:29–35.

Jpn J Radiol (2010) 28:8–14
DOI 10.1007/s11604-009-0373-9

ORIGINAL ARTICLE

Characteristic signal intensity changes on postmortem magnetic resonance imaging of the brain

Tomoya Kobayashi · Seiji Shiotani · Kazunori Kaga
Hajime Saito · Kousaku Saotome · Katsumi Miyamoto
Mototsugu Kohno · Kazunori Kikuchi
Hideyuki Hayakawa · Kazuhiro Homma

Received: May 22, 2009 / Accepted: August 26, 2009

Abstract
Purpose. We investigated and identified postmortem changes on magnetic resonance imaging (MRI) of the brain to provide accurate diagnostic guidelines.
Materials and methods. Our subjects were 16 deceased patients (mean age 57 years) who underwent postmortem computed tomography (CT), MRI, and autopsy, the latter of which showed no abnormalities in the brain. The subjects underwent CT and MRI 6–73 h after confirmation of death (mean 26 h), after being kept in cold storage at 4°C. Postmortem MRI of the brain was performed using T1-weighted imaging (T1WI), T2WI, fluid attenuated inversion recovery (FLAIR) imaging, and diffusion weighted imaging (DWI) with parameters identical to those used for living persons.
Results. In all cases, postmortem CT showed brain edema and swelling. Postmortem MRI showed characteristic common signal intensity (SI) changes, including (1) high SI of the basal ganglia and thalamus on T1WI; (2) suppression of fat SI on T2WI; (3) insufficient SI suppression of cerebrospinal fluid on FLAIR imaging; (4) high SI rims along the cerebral cortices and the ventricular wall on DWI; and (5) an apparent diffusion coefficient decrease to less than half the normal value.
Conclusion. Postmortem MRI of the brain in all cases showed characteristic common SI changes. Global cerebral ischemia without following reperfusion and low body temperature explain these changes.

Key words Postmortem brain CT · Postmortem brain MRI · Postmortem signal intensity change · Global cerebral ischemia · Low body temperature

T. Kobayashi (✉) · K. Kaga · H. Saito · K. Saotome · K. Miyamoto
Department of Radiological Technology, Tsukuba Medical Center, 1-3-1 Amakubo, Tsukuba 305-8558, Japan
Tel. +81-29-851-3511; Fax +81-29-858-2773
e-mail: t.kobayashi1001@gmail.com

S. Shiotani
Department of Radiology, Tsukuba Medical Center, Tsukuba, Japan

M. Kohno
Department of Critical Care and Emergency Medicine, Tsukuba Medical Center, Tsukuba, Japan

K. Kikuchi
Department of Pathology, Tsukuba Medical Center, Tsukuba, Japan

H. Hayakawa
Department of Forensic Medicine, Tsukuba Medical Examiner's Office, Tsukuba, Japan

K. Homma
Advanced Industrial Science and Technology, Human Science and Biomedical Engineering, Tsukuba, Japan

This article was presented at the 94th scientific assembly and annual meeting of the Radiological Society of North America, Chicago, November 2008

Introduction

In the course of the worldwide decline in the conventional autopsy rate, postmortem imaging using computed tomography (CT), magnetic resonance imaging (MRI), and ultrasonography has been used to provide supplementary or complementary information for autopsy.[1–13] In Japan, 90% of large hospitals with emergency room (ER) facilities use postmortem imaging to define or presume the cause of death of patients carried

into the ER in cardiopulmonary arrest on arrival (CPAOA) and whose death was confirmed even though cardiopulmonary resuscitation (CPR) had been performed.[14]

Without knowing the usual findings of postmortem imaging, we cannot interpret whether they are related or unrelated to the cause of death. Diagnostic methods of postmortem CT (PMCT) findings have been established to some extent, regarding causes of death and associated changes,[15,16] postmortem changes,[17–19] and changes after CPR.[20,21] On postmortem MRI (PMMRI), characteristic signal intensity (SI) change has not been reported except for insufficient SI suppression of cerebrospinal fluid (CSF) on fluid attenuated inversion recovery (FLAIR) images due to cooling of the body after death.[22] Yen et al. reported forensic neuroimaging results on PMMRI in 57 postmortem cases, but they did not describe the characteristic SI changes that occurred in the normal brain with no pathology.[23] Herein, we report some common, characteristic SI changes that we noted on PMMRI of the brain.

Methods

Our subjects were 16 deceased adults (male:female ratio 13:3) at 25–87 years of age (mean 57 years) who had all undergone PMCT, PMMRI, and autopsy between October 2007 and March 2009). In all of them the autopsy had shown no abnormalities in the brain. They had presented to the ER in a CPAOA state, and death was confirmed even though CPR was performed. All cases were classified as unexpected and sudden death (occurring within 24 h of the onset of symptoms) due to natural causes.[24] The subjects underwent PMCT and PMMRI 6–73 h after confirmation of death (mean 26 h), after being kept in cold storage at 4°C.

After performing PMCT and PMMRI, the subjects underwent autopsy at the medical examiner's office. The autopsy findings of the causes of death were ischemic heart disease (6 cases), acute heart failure probably due to lethal arrhythmia (3 cases), panperitonitis (2 cases), sepsis (1 case), rupture of the liver (1 case), rupture of an abdominal aortic aneurysm (1 case), pulmonary arterial thromboembolism (1 case), and suffocation (1 case). All subjects were able to perform oral ingestion before death, and there was no case of hereditary disease (e.g., neurofibromatosis) or hepatic disease.

PMCT and PMMRI were performed using clinical scanners for living patients with the permission of the ethics committee of our institution. PMCT was performed with a 16-channel multidetector row CT (MDCT) scanner (Aquilion 16; Toshiba Medical Systems, Tokyo, Japan). The scan parameters for the brain were as follows: conventional scan mode, 120 kV, 200 mA, 2 s/rotation (generally, 1.5 s/rotation for a living person), 1 mm collimation, and contiguous 4-mm sections. PMMRI was performed with a 1.5 tesla (T) MRI scanner (Magnetom Symphony; Siemens, Erlangen, Germany). The scan parameters for the head region were as follows: T1-weighted imaging (T1WI) (TR/TE 540/11 ms, field of view (FOV) 22 cm, matrix 218 × 256, slice/gap 6 mm/1 mm); T2-weighted imaging (T2WI) (TR/TE 4050/118 ms, echo train length (ETL) 11, FOV 22 cm, matrix 230 × 384, slice/gap 6 mm/1 mm); FLAIR imaging (TR/TE/TI 8000/109/2300 ms, ETL 23, FOV 22 cm, matrix 192 × 256, slice/gap 6 mm/1 mm); and diffusion-weighted image (DWI) (TR/TE 3900/105 ms, echo-planar imaging factor 128, b = 1000 s/mm^2, FOV 22 cm, matrix 128 × 128, slice/gap 6 mm/1 mm). These scan parameters are identical to those used for living persons in our institution. A board-certified radiologist evaluated the postmortem imaging findings.

Apparent diffusion coefficient (ADC) maps were automatically generated by DWI, and ADC values were obtained by direct reading of the region of interest in each hemisphere's four distinct neuroanatomical structures (frontal cortical gray matter, frontal white matter, lentiform nucleus, thalamus). The regional variation of ADC values was studied using the Bartlett test to verify the homogeneity of variances and one-way analysis of variance (ANOVA) to compare the means. All tests of significance were two-sided, and a $P < 0.05$ was considered to indicate a significant difference. Statistical analysis was performed using Excel 2003 (Microsoft, Redmond, WA, USA) with the add-in software Statcel 2 (OMS, Tokyo, Japan).

Results

In all subjects, PMCT of the brain showed brain edema with reduced contrast attenuation of the cerebral parenchyma (i.e., obscuration of the gray–white matter interface and lentiform nucleus) and brain swelling with sulcal effacement (Fig. 1). Physiological calcification with aging was seen in two subjects.

PMMRI of the brain showed the following characteristic SI changes in all subjects: On T1WI, the basal ganglia (lentiform nucleus, caudate nucleus) and the thalamus showed higher SI than the white matter (Fig. 2). However, this high SI change was not seen in the hippocampus, the paracentral gyri, or the brain stem. On T2WI, the basal ganglia and thalamus showed low SI, which was almost equivalent to that of the white matter; thus, the SI differentiation was lost between them

(Fig. 3a). The SI of the intraorbital and subcutaneous fat was suppressed on T2WI (Fig. 3b). On FLAIR images, insufficient SI suppression of CSF was seen (Fig. 4). On DWI, high SI rims were seen along the cerebral cortices and ventricular wall, whereas the basal ganglia and thalamus showed slightly low SI compared to that of the surrounding white matter (Fig. 5). On an ADC map, the whole brain parenchyma showed low SI and did not show a low SI rim along the cerebral cortex or ventricular wall to correspond with the DWI findings (Fig. 6). The ADC values were 0.42 ± 0.18 (mean $\pm$ SD) $\times 10^{-3}$ mm^2/s (range 0.18–0.73 $\times 10^{-3}$ mm^2/s)in the frontal cortical gray matter; $(0.29 \pm 0.15) \times 10^{-3}$ mm^2/s (0.1–0.71 $\times 10^{-3}$ mm^2/s) in the frontal white matter; $(0.35 \pm 0.16) \times 10^{-3}$ mm^2/s (0.14–0.69 $\times 10^{-3}$ mm^2/s) in the lentiform nucleus; and $(0.35 \pm 0.14) \times 10^{-3}$ mm^2/s (0.15–0.67 $\times 10^{-3}$ mm^2/s) in the thalamus. The Bartlett test ($P = 0.952$) and ANOVA ($P = 0.569$) indicated no significant differences between these ADC values.

Autopsy did not identify the brain edema observed on PMCT and the causes for SI changes observed on PMMRI. Thus, the pathologists diagnosed that the brains of the subjects had normal aging changes but no pathological states, such as cerebral hemorrhage, infarction, gliosis, demyelination, necrosis, or putrefaction.

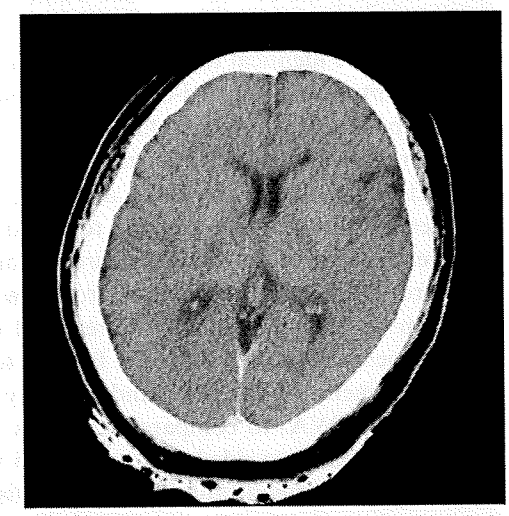

Fig. 1. A 37-year-old woman. Postmortem computed tomography (CT) scan of the brain performed 36 h after confirmation of death shows loss of the gray–white matter interface, obscuration of the lentiform nucleus, and sulcal effacement

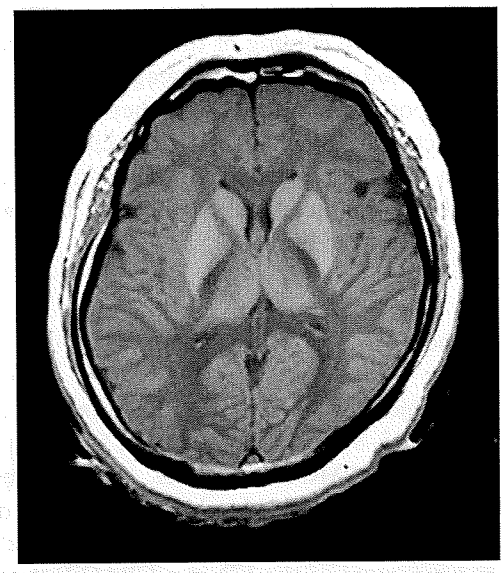

Fig. 2. A 37-year-old woman. Postmortem magnetic resonance imaging (MRI): T1-weighted image (T1WI) of the brain performed 36 h after confirmation of death shows high signal intensity of the basal ganglia and thalamus compared to surrounding white matter

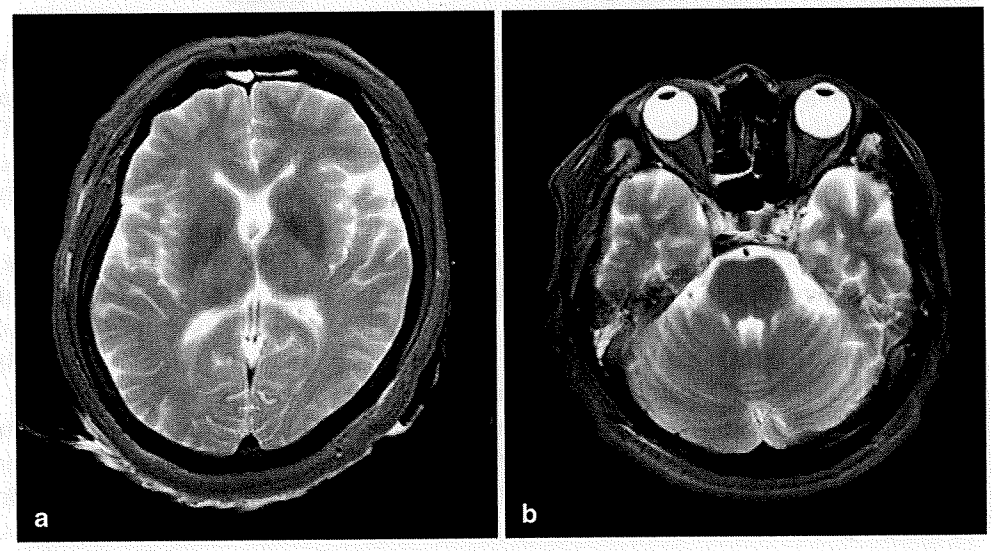

Fig. 3. **a** A 37-year-old woman. T2WI postmortem MRI of the brain performed 36 h after confirmation of death shows low signal intensity across the entire brain parenchyma and an unclear distinction between the gray and white matter. **b** A 66-year-old man. T2WI postmortem MRI of the brain performed 13 h after confirmation of death shows signal suppression of the intraorbital and subcutaneous fat tissue. Low signal intensity in the basilar artery was thought to have occurred not because of a flow void but because of deoxyhemoglobin

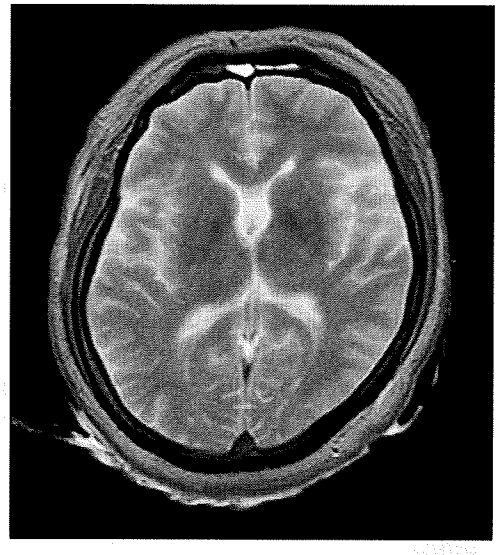

Fig. 4. A 37-year-old woman. Postmortem MRI—fluid attenuated inversion recovery (FLAIR) image—of the brain obtained 36 h after confirmation of death shows insufficient signal suppression of the cerebrospinal fluid

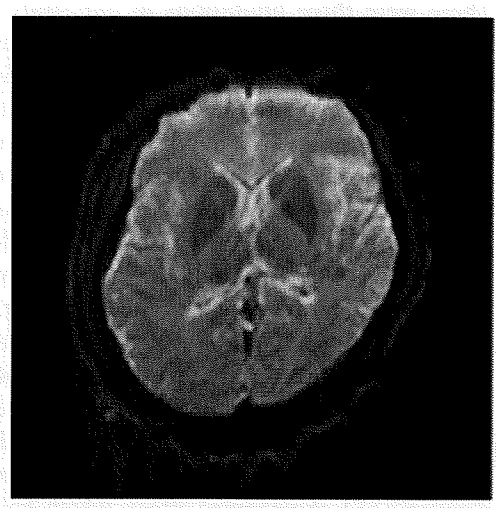

Fig. 5. A 37-year-old woman. Postmortem MRI diffusion weighted image of the brain obtained 36 h after confirmation of death shows high signal intensity rims along the cerebral cortices and the ventricular wall

Discussion

In our study, PMCT of the brain indicated edema, which agreed with the findings of sequential PMCT of the brain that were reported by Sarwar and McCormick.[25] All of our cases were categorized as unexpected, sudden death, before which the patients had undergone sudden global cerebral ischemia, without experiencing a following reperfusion. Based on the staging of cerebral infarction, they were categorized into hyperacute to early acute; thus, the type of this brain edema was cytotoxic.[26,27]

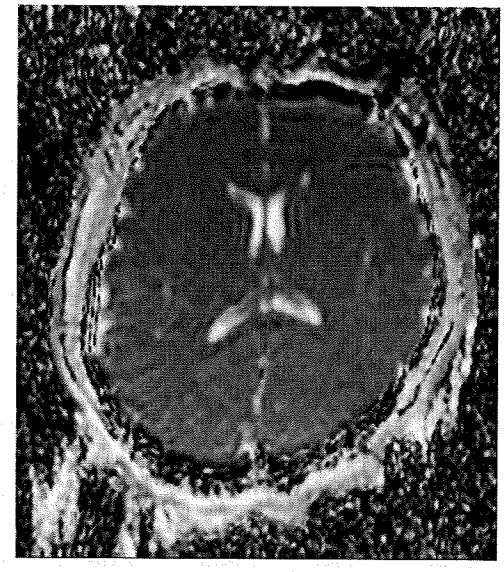

Fig. 6. A 37-year-old woman. Apparent diffusion coefficient map of the brain obtained from postmortem MRI performed 36 h after confirmation of death shows low signal intensity across the entire brain parenchyma.

However, autopsy did not identify the edema that was observed on PMCT. This was probably because the observed edema was slight, and the pathologists decided that the brain was in a normal postmortem state.

With PMMRI of the brain, the basal ganglia and thalamus showed high SI on T1WI. The pathological states of the basal ganglia that might be responsible for the high SI on T1WI were reported to include calcification, parenteral nutrition, portosystemic encephalopathy, and neurofibromatosis.[28] In our study, PMCT findings of physiological calcification with aging were seen in only 2 of the 16 subjects, and none of the subjects exhibited the other three conditions. Generally under such conditions, the thalamus does not show high SI on T1WI. Therefore, those are considered not definitive causes for high SI of the basal ganglia and the thalamus.

Global cerebral ischemia can be a cause of high SI on T1WI of the basal ganglia and thalamus.[29–33] In our study, the basal ganglia and thalamus did display high SI on T1WI, but there were no pathological findings that corresponded with the SI changes. Therefore, the cause of the high SI change was believed to be a functional abnormality that preceded the organic changes (e.g., free radicals induced by hypoxemia, manganese (Mn) accumulation in response to Mn superoxide dismutase (Mn-SOD) as free radical scavenger, iron accumulation associated with the failure of normal axonal transportation).[29–32] However, such a characteristic SI change has been reported to appear 1 week or more after the onset

of brief cerebral ischemia but not in a few days,[30–32] although Mn-SOD and/or iron do start to accumulate within a few to 60 min after cerebral ischemia.[34,35] In our subjects, high SI on T1WI was shown at a mean of 26 h after confirmation of death, which was earlier than previously reported.[30–32] One of the causes is thought to be related to low body temperature because low temperature can shorten the T1 value of the iron component.[36]

On T2WI of PMMRI, fat tissues were shown with low SI. The SI of fat tissues is higher on T2WI with the fast spin echo sequence than that on T2WI with the conventional spin echo sequence.[37] In our study, although we used the fast spin echo sequence for T2WI, fat tissues showed low SI. This can be explained by low body temperature. The correlation time of water molecules varies inversely with temperature. Referencing a graph based on the BPP theory of relaxation (horizontal axis: logarithm of the correlation time; vertical axis: logarithm of T1 and T2 values),[38] when the correlation time is prolonged (= temperature decreases), the T1 value is shorted initially and then prolonged. In ordinary fat tissue, the T1 value is elevated when the correlation time is prolonged because the correlation time of the fat shows a minimum T1 value; whereas when the correlation time is prolonged, the T2 value is shortened linearly. This is why the fat tissue shows low SI only on T2WI of PMMRI.

On FLAIR images of PMMRI, the SI of CSF was insufficiently suppressed, which is also considered to be due to the changes occurring in the body temperature (becoming lower). The T1 value of nonviscous liquid such as CSF is reduced at low temperatures.[38] The null point (= inversion time) to suppress the CSF signal is shortened. Failure to null or suppress the CSF signal results in high SI of CSF on FLAIR images.[22] On FLAIR images of PMMRI, the inversion time needs to be shortened to suppress the CSF signal.

On DWI, high SI rims were seen along the cerebral cortices and the ventricular wall. If the cause was a reduction of diffusion, the region must have shown lower SI than the surrounding parenchyma on an ADC map. However, we did not observe such a finding. Therefore, we believed the cause to be a T2 shine-through effect,[39] although it remains unclear why the T2 value of the corresponding site was prolonged. In our study, the ADC values were reduced to approximately half of the normal values[40] of an adult cerebral cortex, basal ganglia, thalamus, and white matter; however, DWI did not show significantly high SI. In a living person, if the ADC values on DWI decrease in certain areas of the brain, the SI should be high. Brain parenchyma after global ischemia with following reperfusion have been reported to show high SI on DWI in a part or wider areas in the cerebral cortex, basal ganglia, thalamus, white matter, and cerebellum.[41,42] In our subjects, the cause of the absence of high SI on DWI is thought to be global cerebral ischemia without following reperfusion and low body temperature, which induced a reduction in ADC values across the entire brain, thus resulting in no significant ADC value differences among regions.

As far as we know, ADC values on PMMRI have been reported in one case of a 10-month-old child with mitochondrial disorder.[43] In the case, the usual postmortem SI changes in the basal ganglia were not apparent because the child had suffered a hemorrhage in bilateral lenticular nuclei. In contrast, Sener reported that the ADC values in the postmortem brain parenchyma (cortex and white matter) ranged between 0.16 and 0.48 $\times 10^{-3}$ mm^2/s (mean 0.34 $\pm$ 0.05), which agreed with our results.

Limitations

There were three limitations in our study. First, there was no histochemical confirmation. A histochemical study is necessary to confirm that Mn-SOD or iron deposition was really the cause of the basal ganglia and the thalamus having high SI on T1WI of PMMRI. Second, our subjects included sudden death only, and their bodies were kept in cold storage. Characteristic SI changes observed on PMMRI in our study (especially high SI on T1WI) should have been investigated in patients with terminal-stage cancer or other type disease that caused the patient to suffer a long agonal stage, such as those with severe cardiac failure, or subjects not kept in cold storage. We do plan to study those in the near future. Third, we did not investigate SI differences related to hypoxemia or pH change. Oxygen has a paramagnetic (T1 shortening) effect, which has been noted in multiple tissues.[44] Metabolites emerge owing to postmortem decomposition including acids such as lactate[45]; thus, the tissues in a deceased person are thought to have increased acidity. However, we did not measure the oxygen density or pH of the brain tissue; thus, we could not evaluate the effect of hypoxemia or pH change on the SI of PMMRI. Further investigation is necessary to determine such effects.

Conclusion

All deceased patients showed the characteristic common SI changes on PMMRI of the brain under the same scanning parameters as those used for living persons. These SI changes on PMMRI were explained by global